Biomedical Hyperspectral Image Segmentation

Chatla Raviteja

A Gowtham

Biomedical Hyperspectral Image Segmentation

Report submitted to the
SRM University - AP, Andhra Pradesh
For the award of the degree

of

Bachelor of Technology

by

Chatla Raviteja
A Gowtham

Under the guidance of

Dr. Anuj Pradeep Deshpande

DEPARTMENT OF ELECTRONICS AND COMMUNICATION ENGINEERING
SRM UNIVERSITY - AP, ANDHRA PRADESH

MAY 2021

CERTIFICATE OF APPROVAL

Certified that the project report entitled **Biomedical Hyperspectral Image Segmentation**, submitted by

1. Chatla Raviteja(AP20110020003)
2. A Gowtham (AP20110020011)

to the SRM University - AP, Andhra Pradesh, for the award of the degree Bachelor of Technology has been accepted by the examiners and that the students have successfully completed the viva-voce examination held today.

(Dr.)

(Examiner)

(Examiner)

(Examiner)

(Supervisor)

Head of the Department,
Department of ECE

Date:
Place :

<u>CERTIFICATE</u>

This is to certify that the report entitled **Biomedical Hyperspectral Image Segmentation**, submitted by

1. Chatla Raviteja (AP20110020003)
2. A Gowtham (AP20110020011)

to SRM University - AP, Andhra Pradesh, is a record of bona fide work carried out under my supervision and is worthy of consideration for the award of the degree of Bachelor of Technology of the Institute.

Dr.Anuj Pradeep Deshpande

(Supervisor)
Assistant Professor
Department of Electronics and Communication Engineering
SRM University - AP,
Andhra Pradesh - 522502
INDIA

Date:

Place:

Contents

Title Page i

Approvalcert iii

Certificate v

Contents vii

List of Abbreviations ix

List of Figures xi

Abstract xiii

1 Introduction 1
- 1.1 Motivation 2
- 1.2 A Layout of the Report 2
- 1.3 Summary 3

2 Literature Survey 5

3 Methodology 9
- 3.1 Data preprocessing 10
- 3.2 Supervised Classification 12
- 3.3 Unsupervised Segmentation 13
- 3.4 Majority Voting 14
- 3.5 End member and Abundance Extraction 14

4 Results 17
- 4.1 Preprocessed Data: 18
- 4.2 Spectral Signatures of Preprocessed Data: 20
- 4.3 Supervised Classification Maps 21
- 4.4 Unsupervised Segmentation 23
- 4.5 Majority Voting 25
- 4.6 End-member and Abudance Extraction: 28

5 conclusions 31

References **33**
References 33

Appendices **33**

List of Abbreviations

1. HSI - Hyperspectral Imaging
2. PCA - Principal Component Analysis
3. t-SNE - t- distributed Stochastic Neighbor Embedding
4. PCA - Principal Component Analysis
5. KNN - K- Nearest Neighbor
6. RF - Random Forest
7. SVM - Support Vector Machine
8. TMD - Three Maximum Density
9. VCA - Vertex Component Analysis
10. NMF - Non-negative Matrix Factorization
11. HKM - Hierarchical K-Means
12. SSIM - Structural Similarity Index Metric
13. MSE - Mean Square Error

List of Figures

4.1 Raw Images ... 18
4.2 Calibrated Images ... 18
4.3 Brighness Normalized Images ... 19
4.4 Noise filtered Images ... 19
4.5 Data Normalized Images ... 19
4.6 Raw Signature ... 20
4.7 Calibrated Signatures ... 20
4.8 Brightness Normalized Signatures ... 20
4.9 Noise filtered Signatures ... 21
4.10 Normalized Signatures ... 21
4.11 t-SNE Representation ... 21
4.12 PCA Representation ... 22
4.13 Random Forest Classification Map ... 22
4.14 KNN filtered Maps(using t-SNE) ... 22
4.15 KNN filtered Maps(using PCA) ... 23
4.16 K-Means Clustering Map(for Clusters = 5) ... 23
4.17 K-Means Clustering Map(for Clusters = 15) ... 24
4.18 K-Means Clustering Map(for Clusters = 24) ... 24
4.19 Majority voting Map(for Clusters = 5) ... 25
4.20 Majority voting Map(for Clusters = 15) ... 25
4.21 Majority voting Map(for Clusters = 24) ... 26
4.22 Majority voting Map(PCA) ... 26
4.23 TMD map of 012-01 ... 27
4.24 Comaprision of Ground truth map and TMD map obtained by using PCA ... 27
4.25 Spectral Signatures for endmembers ... 28
4.26 Abundance maps ... 28
4.27 Abundance maps ... 29
4.28 Spectral Signatures for endmembers ... 29
4.29 Abundance maps ... 29
4.30 Abundance maps ... 30
4.31 Abundance maps ... 30
4.32 Abundance Map ... 30

Abstract

Accurate tumor segmentation is crucial to the development of neurosurgical procedures for treating brain cancer because it allows for maximum resection with the least amount of damage to healthy tissue. Hyperspectral imaging (HSI) is a promising new method for intraoperative tumor border identification because it is safe, harmless, and passive. Here, we report a new classification scheme that uses the spectral and spatial properties of HSI to help neurosurgeons identify tumors in real time during resection operations. To achieve accurate tumor border delineation, our method combines supervised and unsupervised machine learning techniques in a hybrid architecture. First, a supervised pixel-wise classification using a Random Forest classifier is carried out. Next, spatial homogenization is achieved using K-Nearest Neighbors (KNN) filtering and Fixed Reference t-Stochastic Neighbors Embedding (t-SNE). The research described in this study attempts to take advantage of HSI properties to create a prototype that can distinguish between brain and tumor tissue when performing neurosurgical treatments. A segmentation map is simultaneously produced by unsupervised clustering using the K-Means technique. By using majority voting, the information from both stages is combined and each cluster is assigned to a particular class. In-vivo hyperspectral brain images with glioblastoma tumors show encouraging outcomes when evaluated, producing precise tumor delineation that has been confirmed by experts. Additionally, using the Principal Component Analysis (PCA), we create a pre-processing chain to homogenize spectral signatures and to achieve better accuracy in differentiating between normal and tumor tissues. And performed a technique that takes preprocessed hyperspectral images and extracts endmembers, or representative spectral signatures. To quantify these endmembers' existence in every pixel, we also extracted abundance maps. For the detection of tumor, hyperspectral imaging is useful because it offers extensive spectral information that can show minute variations in tissue composition. Here, we worked on a machine learning-based benchmark to lead further research in in-vivo brain tumor identification and delineation using hyperspectral imaging, which will be utilized as a real-time decision support tool in surgical procedures.

.

Keywords: Hybrid architecture, spectral signatures, Data preprocessing, Brain tumor detection, segmentation.

CHAPTER 1

Introduction

1.1 Motivation

The significant challenges presented by Glioblastoma and other brain tumors, as well as the urgent clinical need to increase the precision of brain tumor delineation during surgery. Due to the shortcomings of current operative imaging methods, novel strategies for real-time, high-resolution tumor localization with the least amount of harm to healthy tissue are required. By offering comprehensive spectral and spatial data, hyperspectral imaging has promise in meeting this demand and may improve the accuracy of tumor delineation. The work intends to close a significant research gap and enhance patient outcomes in brain cancer surgery by creating a novel framework for automated tumor segmentation and classification using hyperspectral imaging. The management of brain cancer could be completely changed if hyperspectral imaging is successfully incorporated into neurosurgical practice and gives neurosurgeons objective, real-time guidance when performing tumor resections. The research intends to improve post-surgery quality of life and patient outcomes by providing surgeons with accurate tumor localization and minimizing damage to healthy brain tissue

1.2 A Layout of the Report

The report is structured in the following way:

- Introduction
- Literature Review
- Methodology
- Results
- Conclusion

1.3 Summary

For intraoperative brain tumor delineation, hyperspectral imaging (HSI) appears to be a potential approach. HSI can distinguish between tumor and normal brain tissue with high accuracy by gathering spectral and spatial data across a broad range of electromagnetic bands. This allows for precise information on the composition of the tissue. This work attempts to create and assess a novel framework for automated tumor segmentation and classification by using the spectral fingerprints of hyperspectral pictures of brain cancer.

To improve the quality and lower the computing complexity of the hyperspectral brain pictures, the proposed system starts with their calibration and pre-processing. Brain tumors are then classified and segmented pixel-by-pixel using sophisticated machine learning methods such as Random Forest classification and K-means clustering. In addition, K-nearest neighbors (KNN) filtering is used to enhance the segmentation outcomes, and Principal Component Analysis (PCA) is employed for feature extraction. Tumor delineation accuracy is further improved by combining supervised and unsupervised classification techniques with a majority vote strategy.And also performed technique that takes preprocessed hyperspectral pictures and extracts endmembers, or representative spectral signatures. To quantify these endmembers existence in every pixel, also create abundance maps. For the detection of tumor, hyperspectral imaging is useful because it offers extensive spectral information that can show minute variations in tissue composition.

The goal of this work is to improve our knowledge of the role that hyperspectral imaging plays in intraoperative brain tumor delineation. This work aims to provide neurosurgeons with objective, real-time guidance during tumor excision procedures by creating a strong and effective framework for tumor segmentation and classification.

CHAPTER 2

Literature Survey

To achieve hyperspectral image segmentation, various methods have been explored in the literature. To increase productivity and reduce complexity, Berkeley wavelet transformation (BWT) was investigated by Bahadure et al. (2017) for the purpose of segmenting brain tumors. Shree Kumar (2018) concentrated on DWT-based segmentation, noise reduction, and gray-level co-occurrence matrix (GLCM) feature extraction for MRI images of brain tumors. The usefulness of thresholding and morphological approaches for brain tumor segmentation was emphasized by Gopalachari et al. in 2022. While Fei et al. (2012) used spectral-spatial classification using LS-SVMs for cancer detection in hyperspectral images, Myasnikov (2017) studied hyperspectral picture segmentation utilizing dimensionality reduction and classical techniques.

Furthermore, Sharma Rattan (2019), concentrating on statistical modelling, presented a segmentation technique for brain cancer diagnosis based on the Hidden Markov Model (HMM). The application of multi-view attention-based ensemble networks for brain tumor segmentation was highlighted by Mushtaq et al. (2022). The efficient identification, segmentation, and detection of tumors in MRI brain images was the focus of Lalitha et al.'s (2020) study. Furthermore, Mahalakshmi Sumathi (2019) talked about content-based active contour segmentation and mean shift clustering as brain tumor segmentation techniques. Together, these studies show the wide range of methods used for morphological operations, statistical modelling, ensemble networks, wavelet transformations, feature extraction, thresholding, dimensionality reduction, and spectral-spatial classification in hyperspectral image segmentation. Every technique advances the field of precise and effective hyperspectral image segmentation for uses like the identification of brain tumors.

Numerous methods and algorithms have been put forth in the literature to segment hyperspectral pictures for the purpose of detecting brain tumors. When it comes to recognizing and defining tumor locations in medical images—especially brain MRI scans—image segmentation is an essential stage. Numerous segmentation techniques have been investigated, including machine learning algorithms, fuzzy logic-based methods, watershed segmentation, and thresholding.

In their discussion of the application of histogram thresholding to the identification of brain tumors, Noureen Hassan (2014) emphasized the significance of picture segmentation. To detect tumors in MRI brain images, Baghel Kirar (2015) emphasized the importance of segmentation followed by morphological operations. While Mustaqeem et al. (2012) suggested a watershed and thresholding-based segmentation method for brain tumor diagnosis, K.S et al. (2019) presented a modified K-Means technique for automatic brain tissue segmentation. A Hybrid GrabCut Hidden Markov Model for brain image segmentation with an emphasis on tumor evaluation was presented by Saeed et al. in 2022.Additionally, watershed segmentation was used by Shanthakumar, Ganeshkumar Ragupathy, and Karunakaran (2020) to detect tumors in brain MRI images. Anitha Raja (2017) segmented brain tumors using a random forest classifier. A unique Woelfel Filter and Morphological Segmentation technique for brain tumor identification was developed by Gopalachari et al. in 2022. Furthermore, the U-Net model for brain tumor segmentation in MRI data was presented by Mridha et al. (2022).

Ma et al. (2022) researched the use of morphological profiles in hyperspectral image segmentation techniques, whereas Myasnikov (2017) investigated the use of dimensionality reduction methodologies in hyperspectral picture segmentation. Fei et al. (2012) used support vector machines and spectral-spatial classification to detect cancer in hyperspectral images. Together, these studies show the wide range of methods used for morphological operations, statistical modelling, ensemble networks, wavelet transformations, feature extraction, thresholding, dimensionality reduction, and spectral-spatial classification in hyperspectral image segmentation. Every technique advances the field of precise and effective hyperspectral image segmentation for uses like the identification of brain tumors. Overall, a wide variety of segmentation techniques for brain tumor identification in hyperspectral and MRI images are available in the scientific literature, demonstrating ongoing efforts to improve the precision and efficiency of tumor segmentation algorithms in medical imaging

CHAPTER 3

Methodology

In-vivo HS Human Brain database is utilized for this project which consists of three campaigns. The total of 61 images are presented in these three campaigns. The hyperspectral (HS) images from 34 distinct patients comprised the dataset, which was created with the goal of detecting brain tumor during surgery. These sixty- one high-strength photos were carefully taken to enable the production of ground-truth maps that are necessary for further examination. The HS pictures cover a spectral range of 440 nm to 900 nm. Each file of these sixty-one images is consists of raw and header files of original HS image, dark reference, white reference, and ground truth maps.

A hybrid architecture is followed to perform the segmentation of HS image for tumor detection. we perform supervised classification and unsupervised segmentation is applied to achieve the better accuracy. Before applying them, the data should be preprocessed

3.1 Data preprocessing

The HS images often contain various types of noise and distortions due to factors like sensor limitations and environmental conditions. By applying preprocessing techniques, we can improve the quality of the data, making it more suitable for further analysis. By using the six steps we preprocessed the data for better feature extraction. The steps are

1. **Calibration:** Actually, the calibration is carried out to prevent the interference from both the HS sensor's dark currents and the illumination of the ambient surroundings. A substance that reflects 99% of the incoming radiation over the whole spectral range was used to create the white reference image. And the camera shutter was kept closed to obtain the dark reference image. So, the calibration is done according to the equation (3.1), where the CI is Calibrated Image, Dr is Dark Reference and Wr is White Reference.

$$CI = 100 * \frac{(Ri - Dr)}{(Wr - Dr)} \tag{3.1}$$

2. **Extreme band removal:** In hyperspectral imaging, spectral bands with high noise levels—typically found at the extremes of the sensor's spectral range—are eliminated through the technique of extreme band removal. By eliminating bands impacted by poor sensor performance, this modification seeks to improve the quality of hyperspectral data. When these noisy bands are removed, the dataset gets cleaner and has less bands, which produces spectral information that is more trustworthy for analysis. For applications such as brain cancer diagnosis, this preprocessing step is crucial because it guarantees that the hyperspectral data used is high quality and free from distortions due to sensor noise, which improves the accuracy of future analysis. So we removed the first 56 and the last 126 spectral channels. Thus, the image is reduced to 645 bands from 826 bands.

3. **Band averaging:** Hyperspectral Imaging (HSI) is a technique that helps identify materials based on their chemical makeup by capturing comprehensive spectral information across a wide range of narrow bands. Through the reduction of its dimensionality, band averaging preserves important information while attenuating noise in the data. Machine learning methods perform better when noise is reduced, like in the case of tumor diagnosis during surgery, by averaging reflectance values across adjacent spectral bands. Additionally, this is a dimensionality reduction of the HS cube was performed by decimating the spectral channels to reduce redundant information in the HS data due to the high dimensionality. The HS image is averaged by 5 resulting in the band reduction from 645 to 129.

4. **Brightness Normalization:** After the successful completion of band averaging, to preserve the spectral properties of the pixels while uniforming their brightness throughout the image. This is important because different surgical procedures can result in different radiation intensities, which can change the brightness of pixels in tumor and normal tissue areas. The brightness of each pixel is determined and each pixel is divided by its brightness value as part of the normalization process, which makes sure that the brightness

levels are constant across the image. Consequently, the classifier may now concentrate on spectral signatures instead of brightness disparities, allowing for a more precise spectral property-based separation of tumor from normal tissues. The equation (3.2) is used to normalize the brightness of the image where P_{BC} is brightness corrected pixel, P is pixel to be corrected and p_i is i^{th} component of this pixel P.

$$P_{BC} = \frac{P}{\sqrt{\sum_{i=1}^{129} p_i^2}} \tag{3.2}$$

5. **Noise Filtering:** To reduce the unwanted random noise in the spectral signature of the hyperspectral image we use smoothing filter. for this, the Gaussian filter is used with the sigma value 1

6. **Data Normalization:** The application of brightness normalization will reduce the reflectance values of spectral signatures from range of 30 and 60 to 0 and 0.1 which are very low to differentiate the tissue properties. So, the HS image must be normalized between [0,1] with the minimum value of 0 and maximum value of 1, in order to homogenize reflectance levels in each pixel of the HS image produced by the non-uniform surface of the brain. The normalization is done based on the equation (3.3) where N'_i is normalized pixel , N_i is the pixel to be normalized at certain wavelength, N_min is minimum reflectance value of pixel and $N_max$is maximum reflectance value of pixel.

$$N'_i = \frac{N_i - N_{\min}}{N_{\max} - N_{\min}} \tag{3.3}$$

3.2 Supervised Classification

As we working based on the hybrid architecture, which means we used both supervised and unsupervised classifications for better segmentation. So, to achieve that we need a classified spatial/spectral classification map, which contains the combined spatial information and spectral information obtained after

performing supervised classification. In supervised, the process involves mainly three

1. One band representation 2. Random forest classification 3.KNN filtering

For one band representation of the preprocessed HS image, we do not need to band averaging of the image because it may result in removing the useful features. So, we consider preprocessed image without band averaging. The features of all 645 bands should be represented in one band for computational efficiency. In this project we used both t-Stochastic Neighbors Embedding (t-SNE) and Principal Component Analysis (PCA). PCA, is a method for reducing data by concentrating on its key components. Although tiny details may be overlooked, it is effective at displaying broad trends in the data. However, t-SNE, excels in highlighting minute patterns and clusters within the data. It is similar to using PCA to see the big picture as opposed to t-SNE to zoom in on specific features. Now, with the initial preprocessed image (which involves band averaging) must be classified with the ground truth image provide in the data set. we used Random Forest (RF) classifier which give accuracy of 99% while comparing with SVM which is proposed by the literature survey. we get a classification map after RF classification. Later, KNN filtering incorporates spatial features to enhance the supervised classification maps generated from spectral data alone. The KNN filtering is applied on one band representation using classification map. This method smooths image, providing more homogeneous class regions and reducing misclassified pixels which gives us spatial/spectral classification map.

3.3 Unsupervised Segmentation

For unsupervised segmentation of preprocessed image, K-means clustering is used instead of HKM (Hierarchical K-Means), which was proposed in the literature review. With each cluster represented by its centroid, K-means clustering seeks to separate the data into a predefined number of clusters. To place data points closest to the nearest centroid, iteratively minimizes the within-cluster variation. However, by establishing a hierarchical structure of clusters, HKM clustering expands on the

idea of K-means. It enables a more thorough segmentation method by identifying regions in hyperspectral pictures based on comparable spectral properties. In the spatial-spectral domain, HKM is especially helpful for unsupervised segmentation. And also, K-means clustering is efficient of computational time reduction and givessimilar results to HKM clustering.

3.4 Majority Voting

Its main goal is to improve the precision of locating and defining brain tumors when doing surgery. Majority Voting uses unsupervised segmentation and supervised classification to assign classes to clusters according to most pixels in each cluster. Tumor separation becomes more accurate as a result of the reduction of false positives and negatives. The end result is a comprehensive map that neurosurgeons can use to identify tumor tissue from normal tissue and blood arteries during surgery. As a visualization tool, this color-coded map helps surgeons make well-informed decisions to maximize tumor excision while minimizing harm to good tissue. For further study we can also use the endmembers and abundance extraction method.

3.5 End member and Abundance Extraction

We can also segment the hyperspectral brain image using the extraction method of endmembers and abundance maps. It uses the preprocessed image and firstly it will extract the endmembers. Next, it uses Non-negative Matrix Factorization (NMF) to estimate abundances, assisting in the identification of the presence and distribution of various materials in the image. Plotting abundance maps allows one to see how endmembers are distributed throughout the image. And also carries out the NFINDR method, which chooses endmembers from the hyperspectral image iteratively according to their spectral properties. Lastly, it plots the chosen endmembers spectral signatures and stores them in a.mat file for later examination. For extraction we have used N-FINDR (Non-negative Factorization with Dynamic

Residuals). By maximizing the volume of the simplex that the endmembers form in spectral space, the iterative N-FINDR algorithm finds endmembers. It accomplishes this by repeatedly choosing pixels that maximize the simplex's volume. Since N-FINDR is more resilient and can accommodate mixed pixels, it is appropriate for a wider range of applications than VCA, which implies pure pixels, which may not always hold true in real-world circumstances.

CHAPTER 4

Results

4.1 Preprocessed Data:

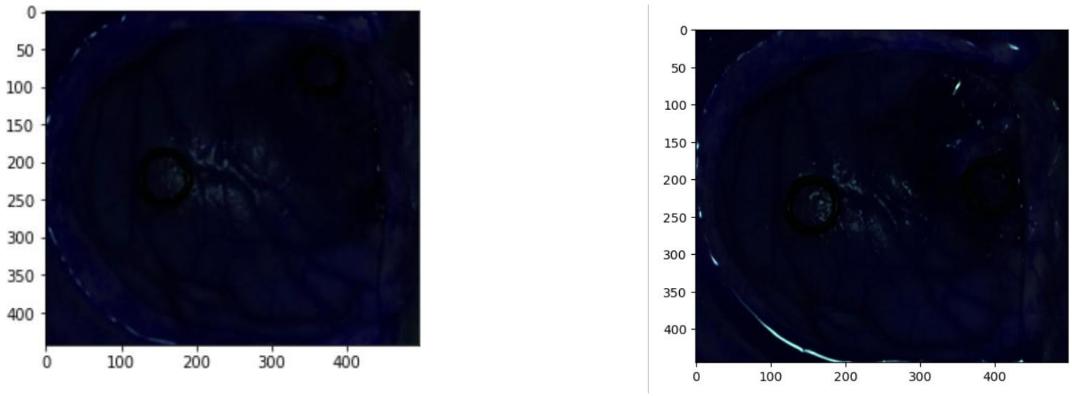

(a) 012-01 (b) 012-02

Figure 4.1: Raw Images

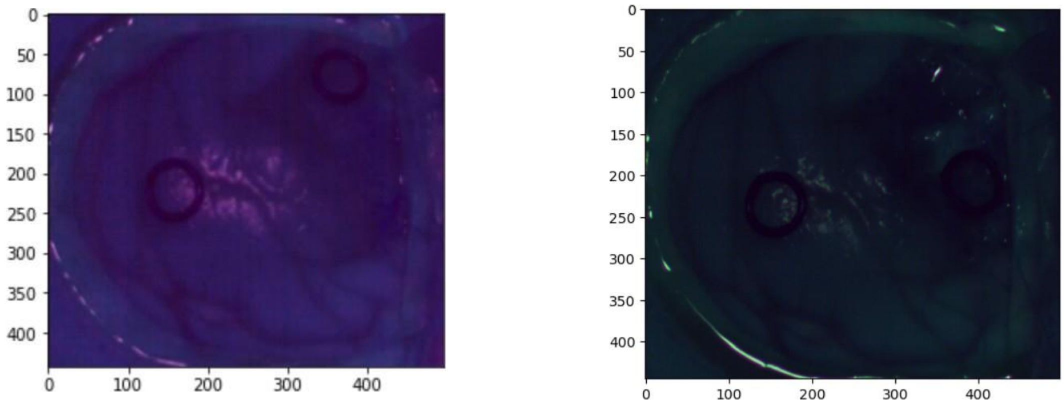

(a) 012-01 (b) 012-02

Figure 4.2: Calibrated Images

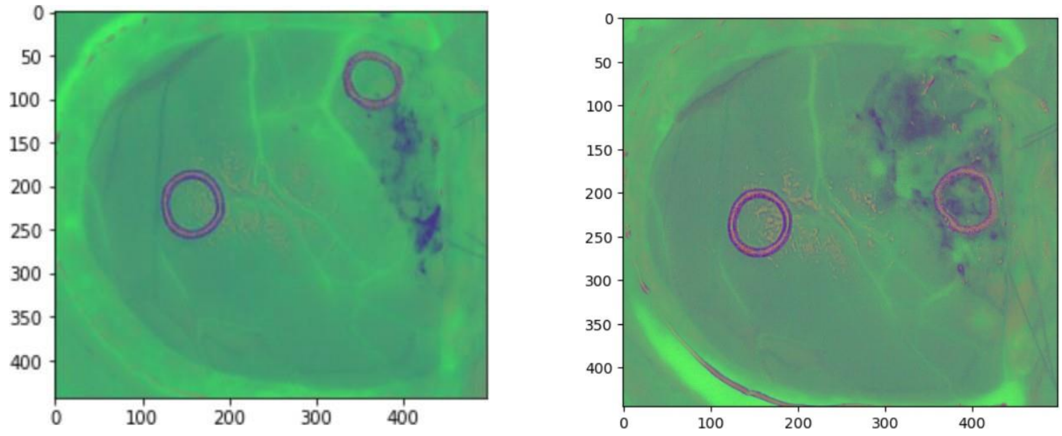

(a) 012-01 (b) 012-02

Figure 4.3: Brighness Normalized Images

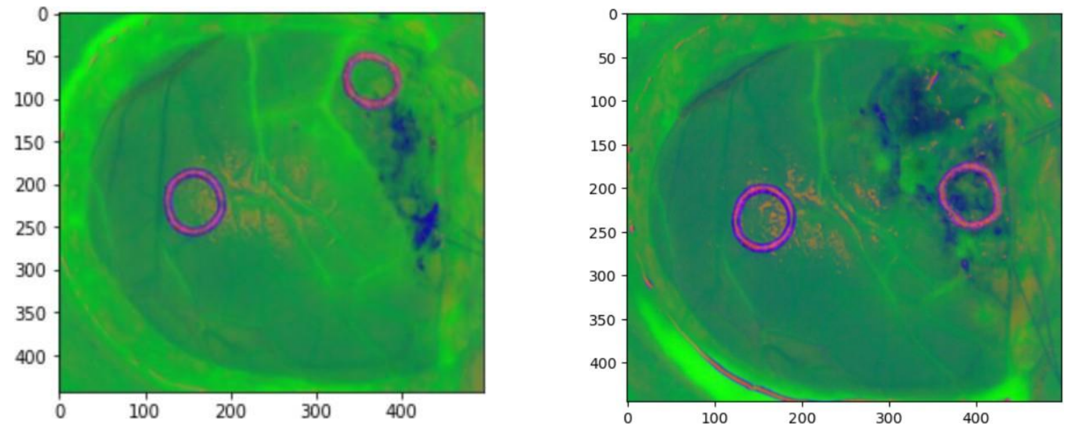

(a) 012-01 (b) 012-02

Figure 4.4: Noise filtered Images

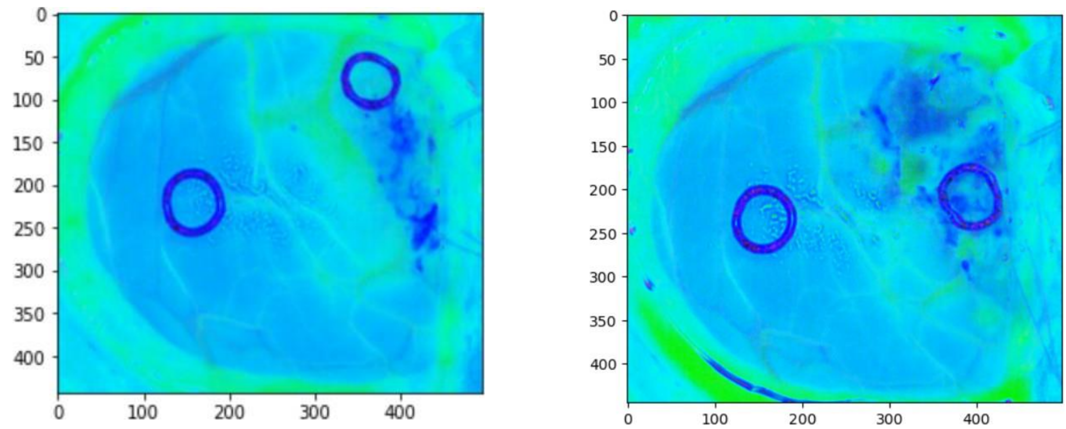

(a) 012-01 (b) 012-02

Figure 4.5: Data Normalized Images

4.2 Spectral Signatures of Preprocessed Data:

These are the spectral signatures of the images at pixel location [100,200]. We can consider any pixel location. These signatures tells whether the image is preprocessed through the representation of reflectance signals.

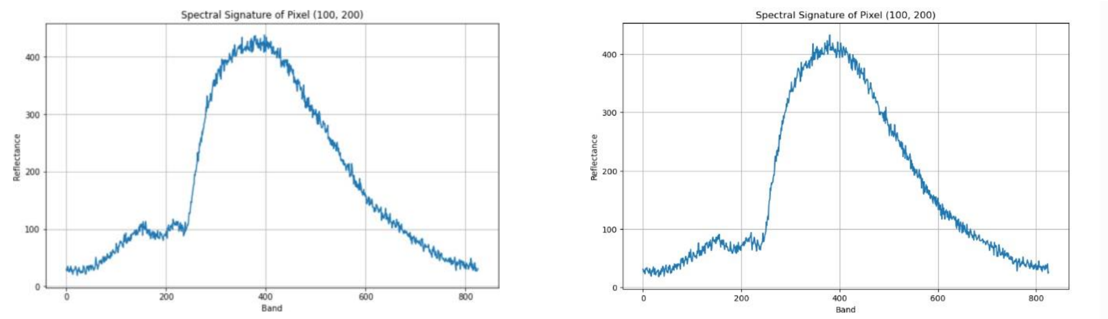

(a) 012-01 (b) 012-02

Figure 4.6: Raw Signature

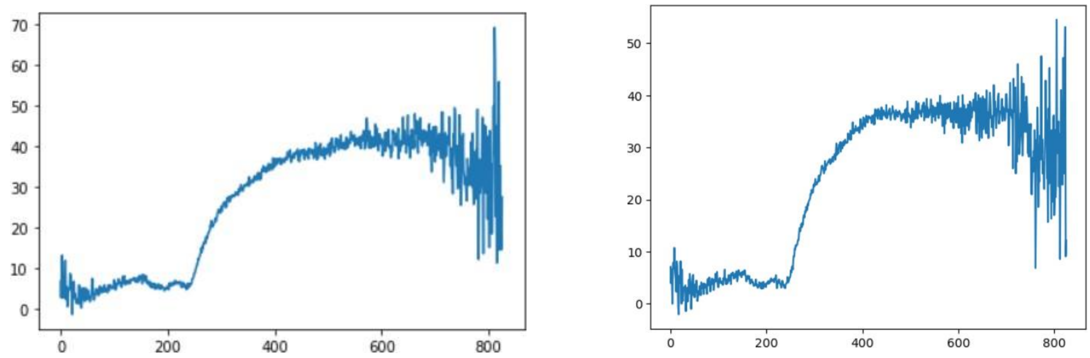

(a) 012-01 (b) 012-02

Figure 4.7: Calibrated Signatures

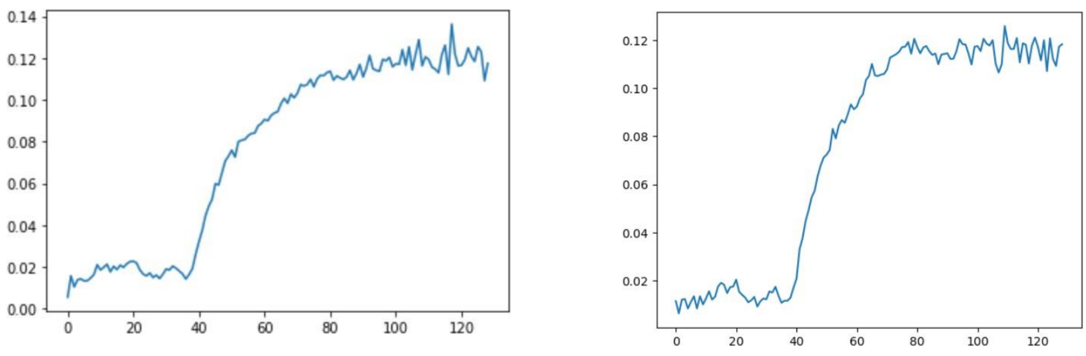

(a) 012-01 (b) 012-02

Figure 4.8: Brightness Normalized Signatures

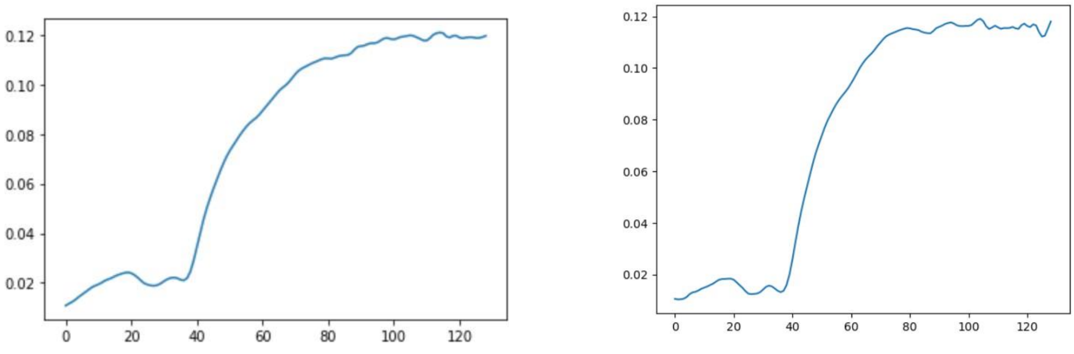

(a) 012-01 (b) 012-02

Figure 4.9: Noise filtered Signatures

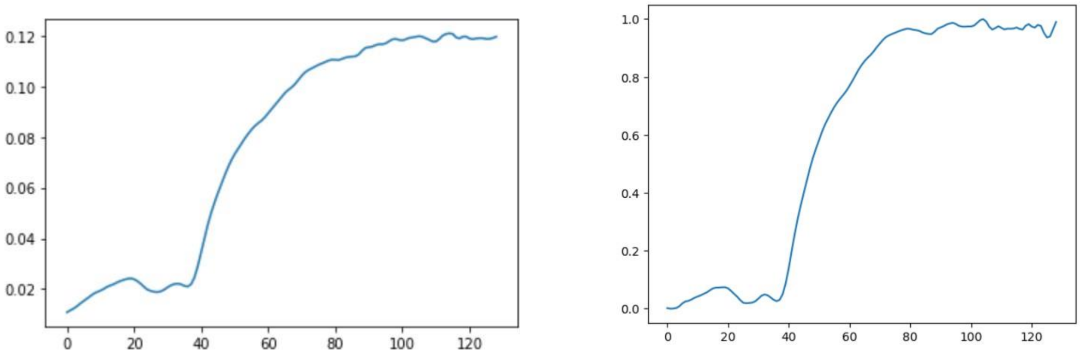

(a) 012-01 (b) 012-02

Figure 4.10: Normalized Signatures

4.3 Supervised Classification Maps

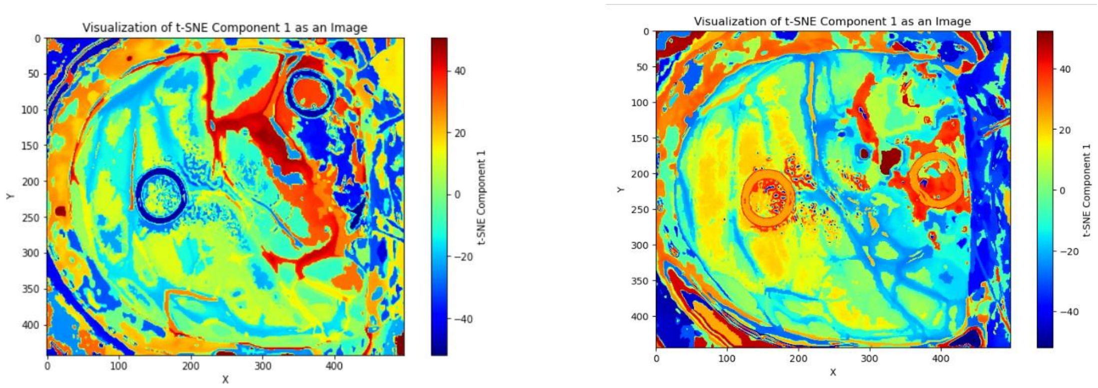

(a) 012-01 (b) 012-02

Figure 4.11: t-SNE Representation

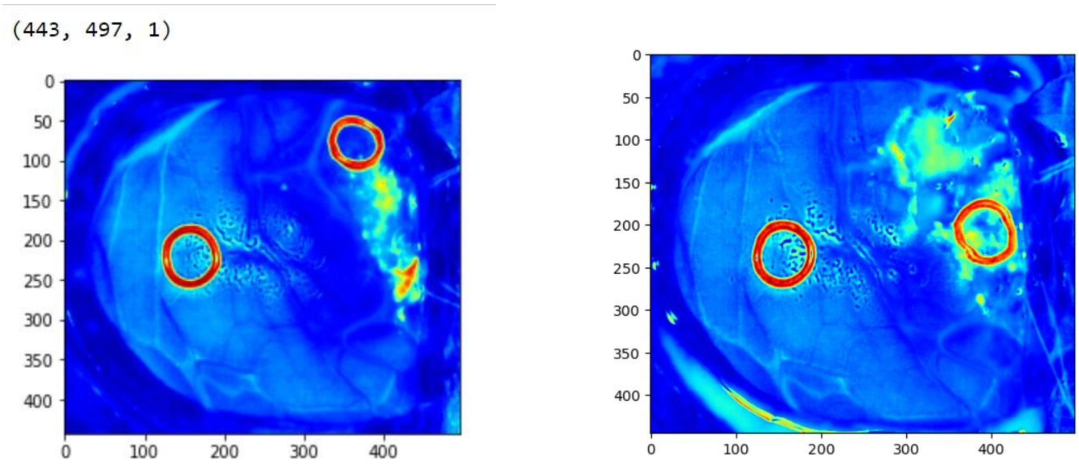

(a) 012-01 (b) 012-02

Figure 4.12: PCA Representation

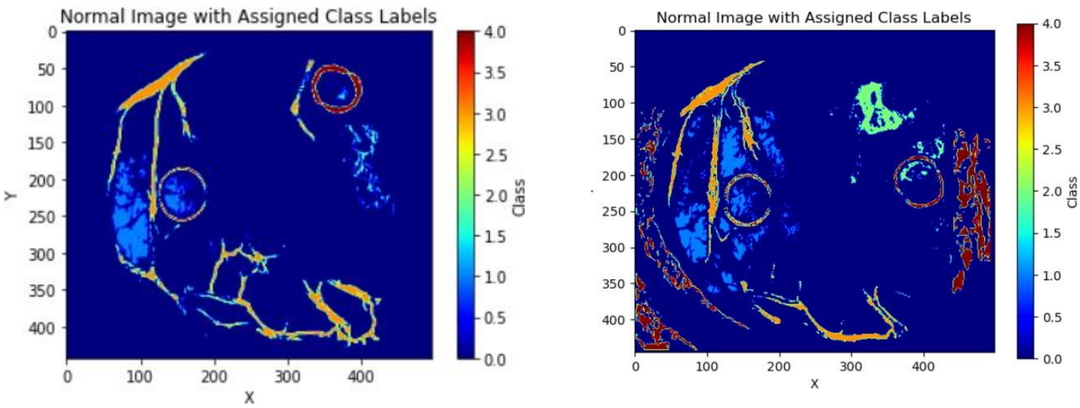

(a) 012-01 (b) 012-02

Figure 4.13: Random Forest Classification Map

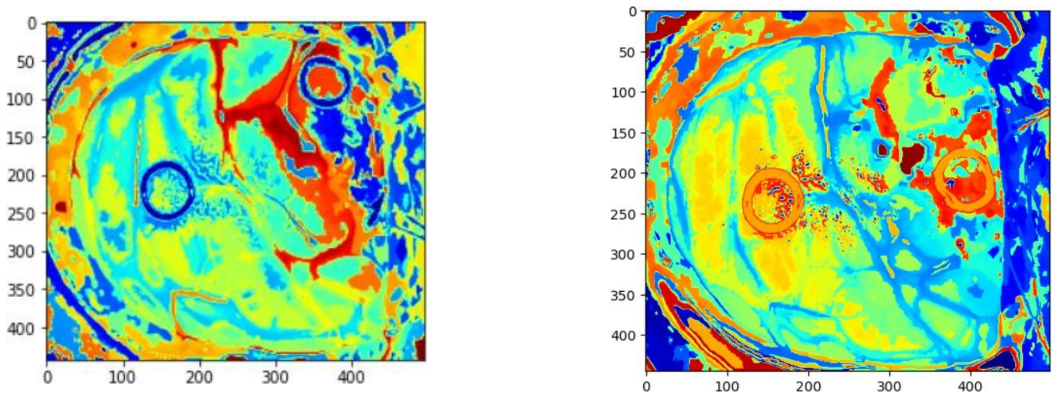

(a) 012-01 (b) 012-02

Figure 4.14: KNN filtered Maps (using t-SNE)

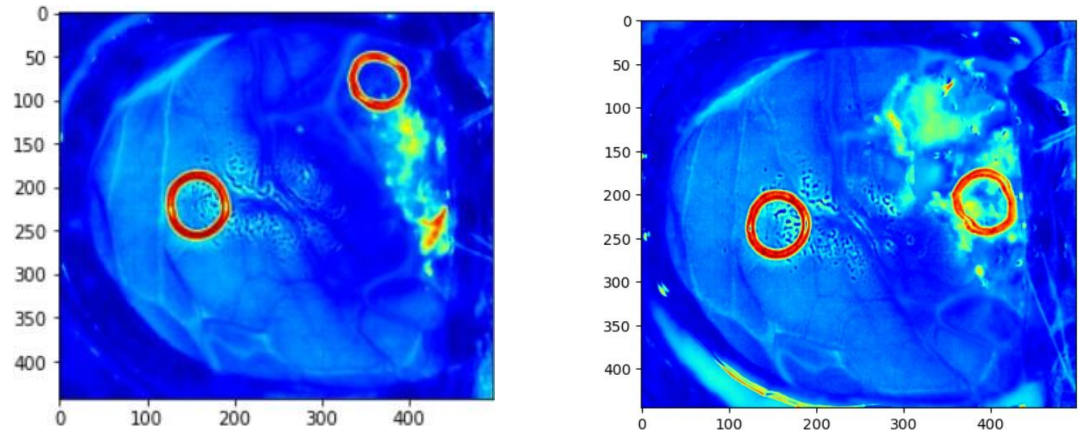

(a) 012-01 (b) 012-02

Figure 4.15: KNN filtered Maps (using PCA)

4.4 Unsupervised Segmentation

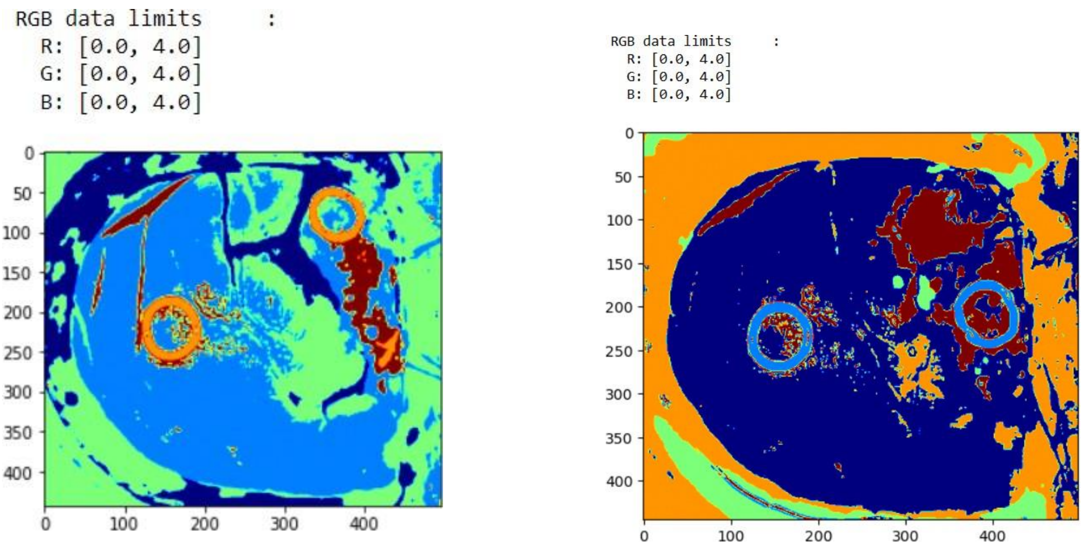

(a) 012-01 (b) 012-02

Figure 4.16: K-Means Clustering Map (for Clusters = 5)

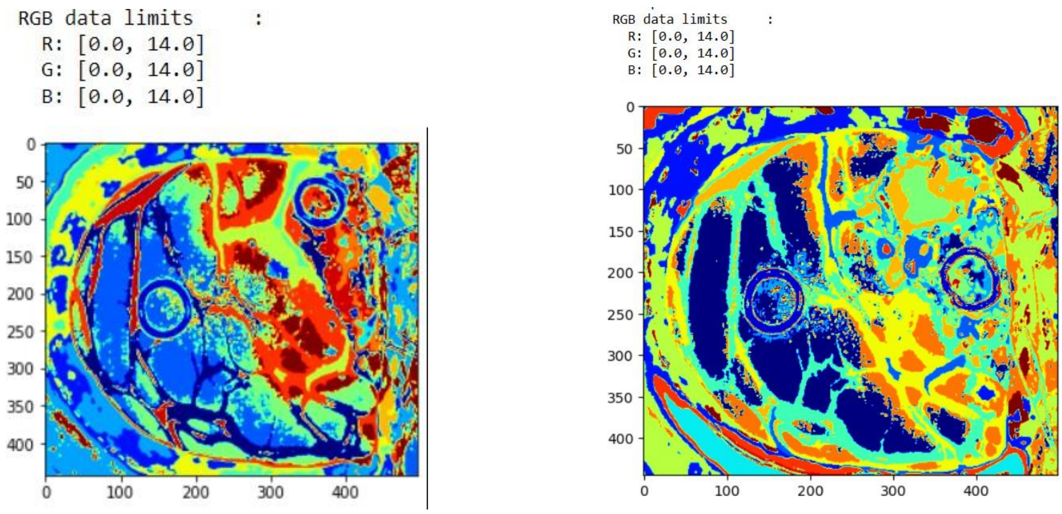

(a) 012-01 (b) 012-02

Figure 4.17: K-Means Clustering Map(for Clusters = 15)

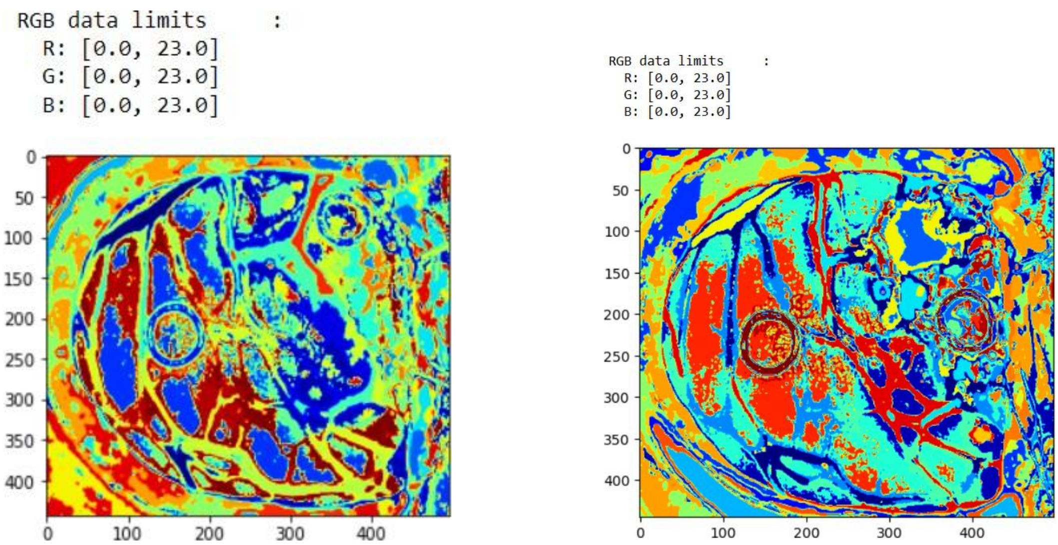

(a) 012-01 (b) 012-02

Figure 4.18: K-Means Clustering Map (for Clusters = 24)

4.5 Majority Voting

The process of Majority voting is done for both t-SNE and PCA representations individually. So the mentioned below are the individual results of majority voting for t-SNE and PCA

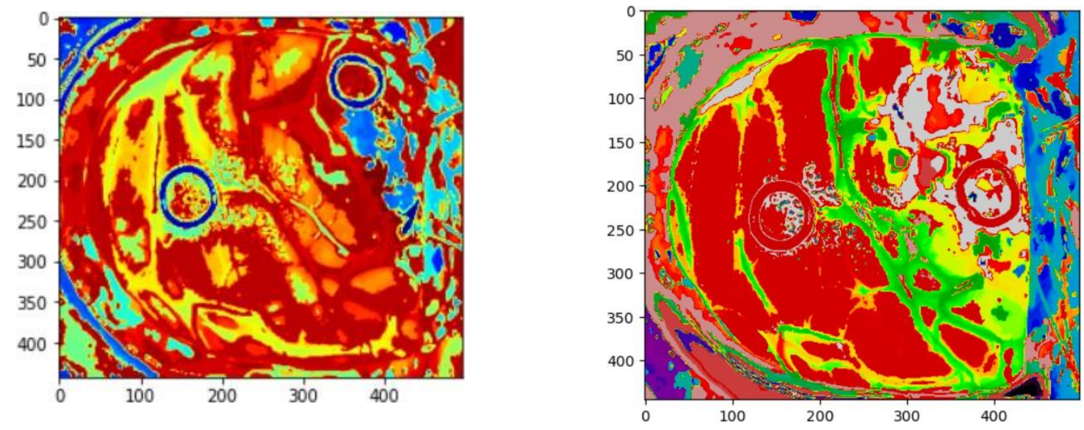

(a) 012-01 (b) 012-02

Figure 4.19: Majority voting Map(for Clusters = 5)

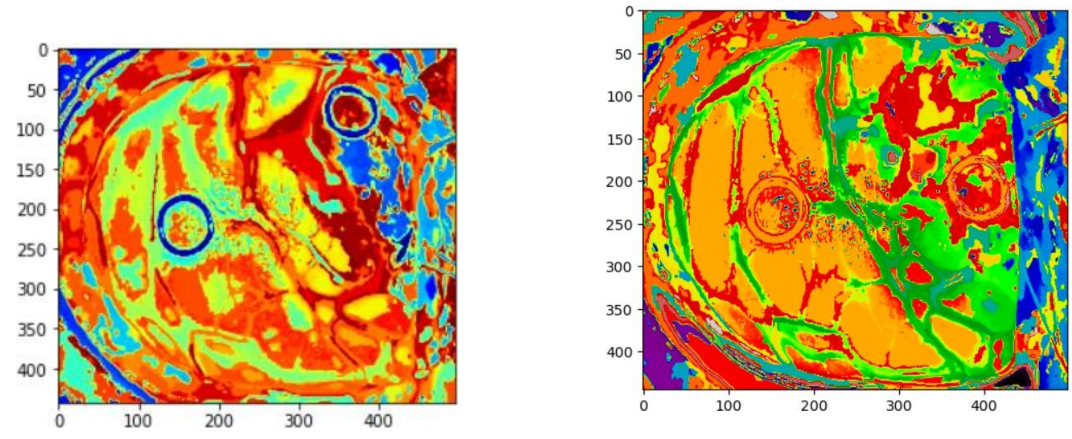

(a) 012-01 (b) 012-02

Figure 4.20: Majority voting Map (for Clusters = 15)

If we take PCA images for KNN filtering, then the below are the results of majority voting

So, the final TMD Three Maximum Density maps, are important when it comes to hyperspectral imaging (HSI)-based brain tumor detection. These maps combine spectral and spatial information from HSI to visually depict brain tumor during surgical procedures. Different tissue types can be identified by using RGB colors, where each color channel represents a certain class, such as blood vessels, tumortissue, and normal tissue.

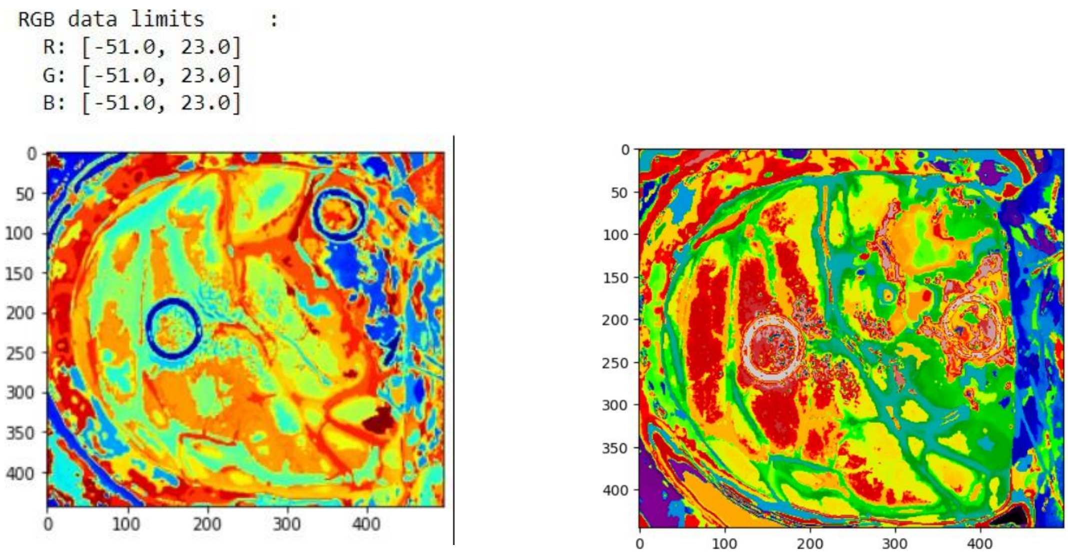

(a) 012-01 (b) 012-02

Figure 4.21: Majority voting Map(for Clusters = 24)

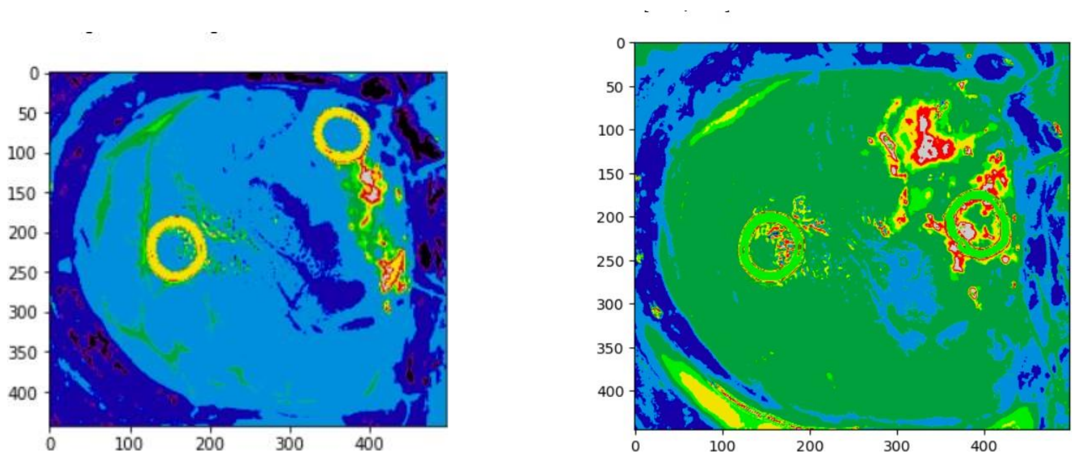

(a) 012-01 (b) 012-02

Figure 4.22: Majority voting Map (PCA)

tumour infiltration into surrounding healthy brain tissue and to correctly delineate tumour boundaries in real time. TMD mapping techniques are being refined with the goal of improving patient outcomes and surgical precision through ongoing optimisation and clinical validation efforts. The final TMD map obtained is

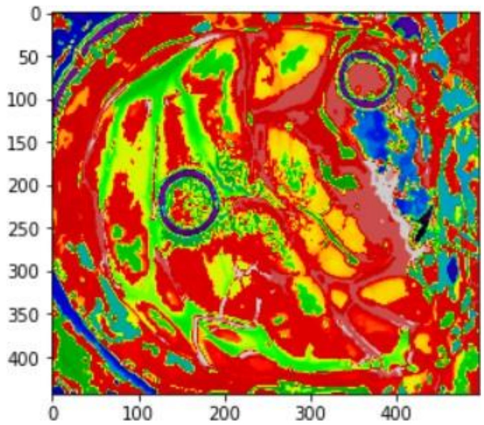

Figure 4.23: TMD map of 012-01

And also to replicate the ground truth during my process PCA have shown the SSIM(Structural Similarity Index Measure) of 0.99 for both 012-01 and 012-02 images and Calculated MSE (Mean Square Error) is 1.179 and 2.256 respectively. As the ground truth are not the ultimate result to calculate the accuracy . Ground truth are mapped by the pathologists which they specified the four Classes which are Normal tissue , Tumor tissue, hypervascular tissue and remaining all as Back ground.The pathologists specified that these are the sure pixel of particualar class manually.

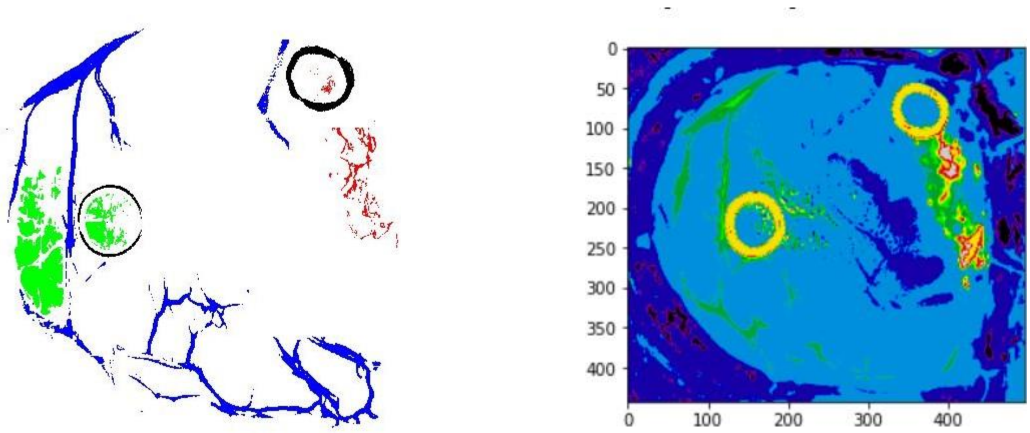

(a) 012-01 (b) 012-01

Figure 4.24: Comparison of Ground truth map and TMD map obtained by using PCA

4.6 End-member and Abundance Extraction:

Here we calculated the endmembers and abundance map for 4 endmembers and for 7 endmembers. Below are the results of them. As we only checked with this process, we need further research to do more on this method. So, these are the intermediate results of the endmembers and abundance extraction for study purpose.

- **For Endmembers = 4, the abundance maps are**

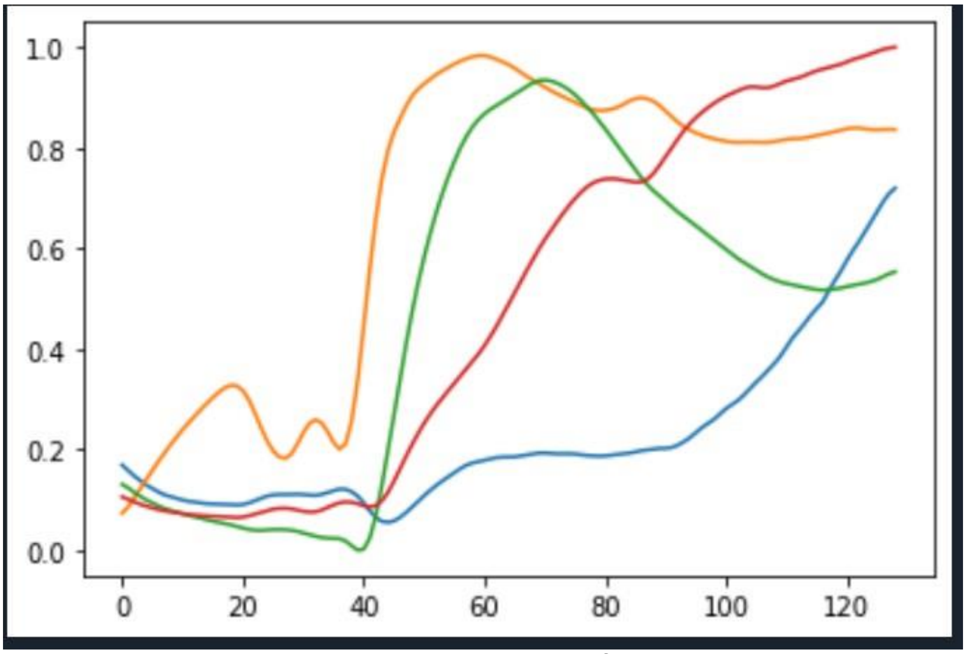

Figure 4.25: Spectral Signatures for endmembers

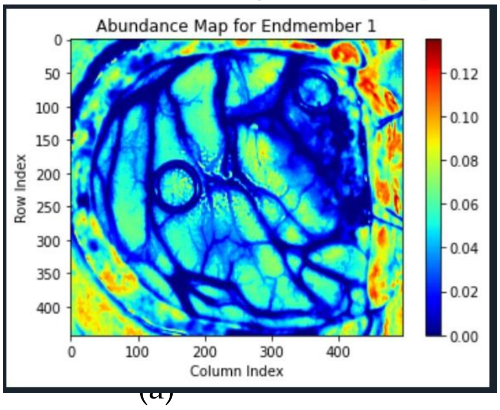

(a) Endmember 1

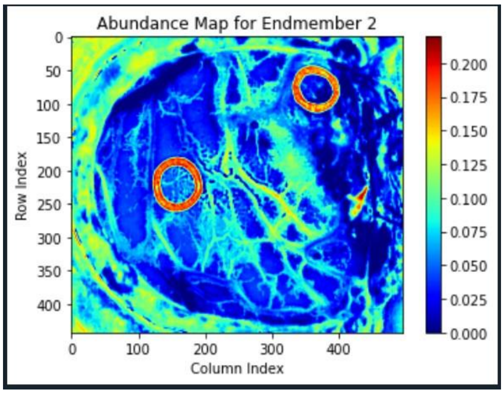

(b) Endmember 2

Figure 4.26: Abundance maps

- **For endmembers = 7, the abundance maps are**

4.6 End-member and Abundance Extraction:

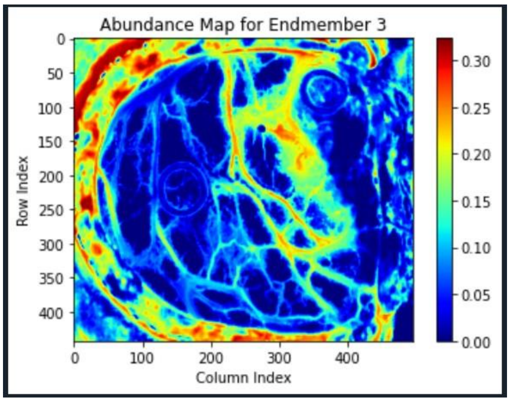

(a) Endmember 3

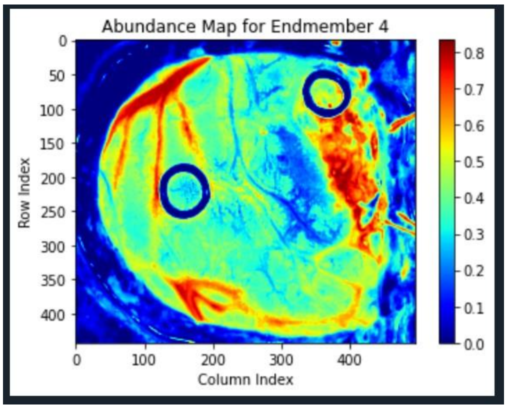

(b) Endmember 4

Figure 4.27: Abundance maps

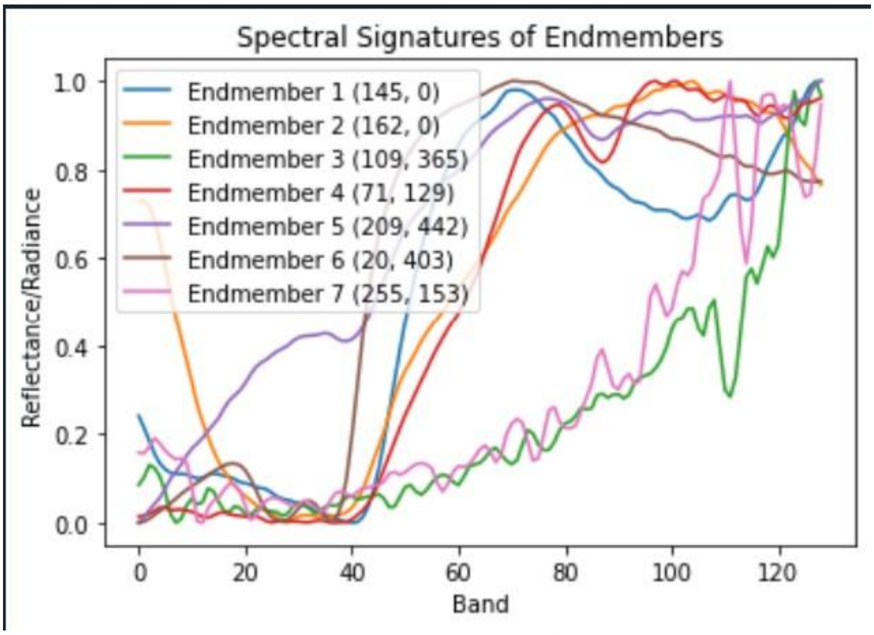

Figure 4.28: Spectral Signatures for endmembers

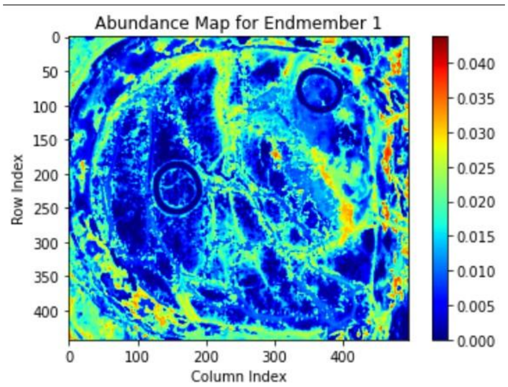

(a) Endmember 1

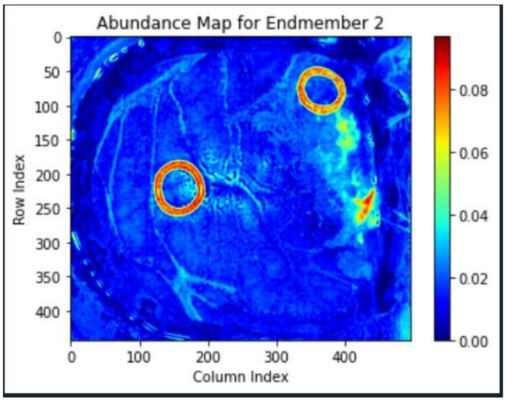

(b) Endmember 2

Figure 4.29: Abundance maps

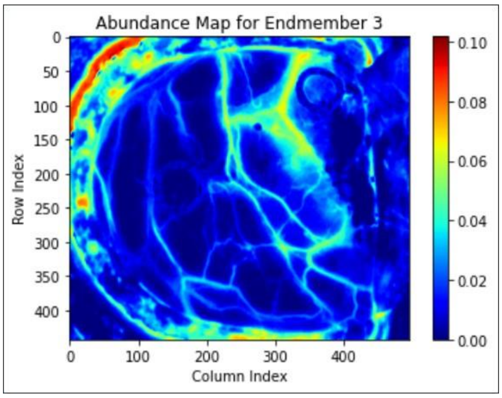

(a) Endmember 3

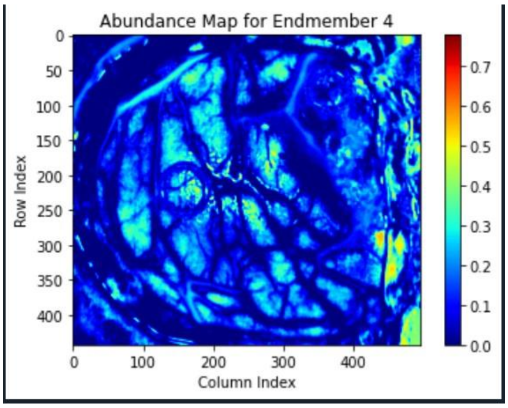

(b) Endmember 4

Figure 4.30: Abundance maps

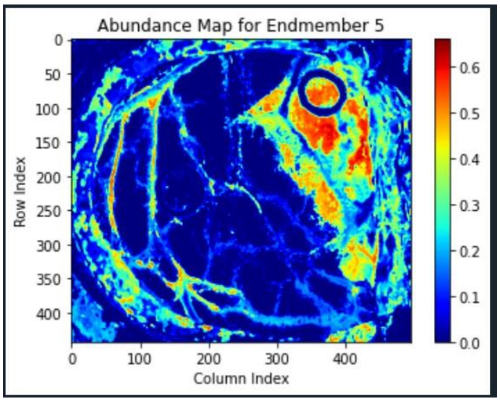

(a) Endmember 5

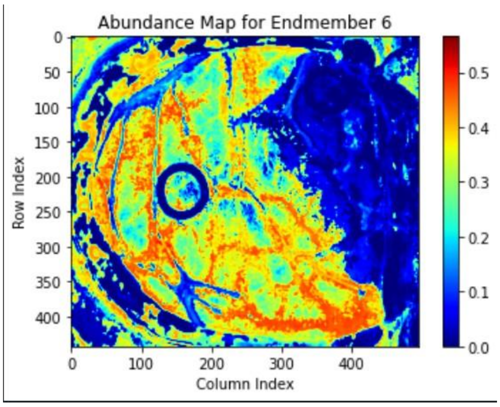

(b) Endmember 6

Figure 4.31: Abundance maps

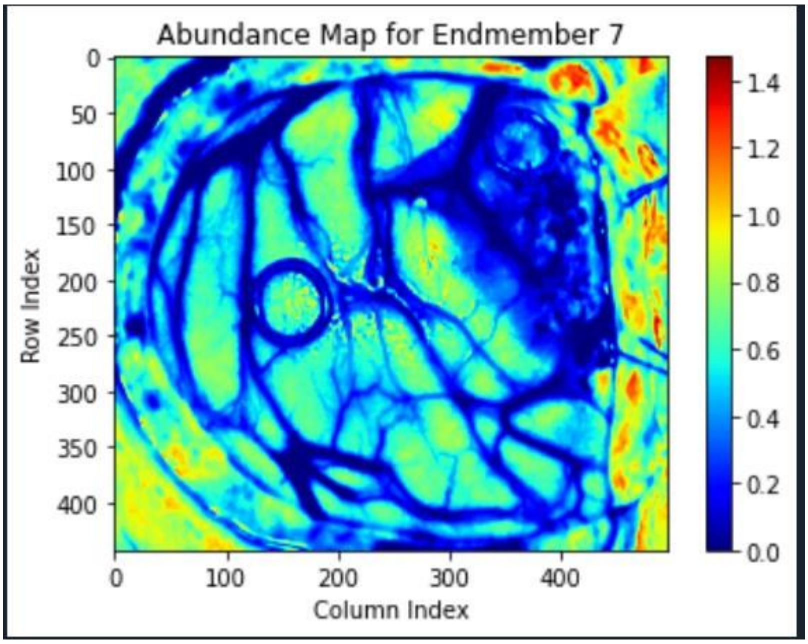

Figure 4.32: Abundance Map

CHAPTER 5

conclusions

In order to classify hyperspectral (HS) images of brain tumor in real-time during neurosurgical procedures, this work presents an algorithm for the diagnosis of brain cancer. The program helps neurosurgeons remove tumor by using Hyperspectral Imaging (HSI) as a new non-invasive tool. This could improve patient outcomes. To minimize needless tissue removal and prevent leaving residual tumor, accurate delineation of tumor boundaries and identification of tumor infiltration into normal brain tissue are essential. Research is still being done to confirm the algorithm's efficacy, generalize and optimize it, With the ability to create numerous TMD maps per second, this development in medical HSI systems may offer neurosurgeons an invaluable real-time visualization tool to assist them throughout the tumor removal procedure. This work provides a study of how can be a Hyperspectral Brain image can be segmented using hybrid architecture and further study is needed to improve this model for better detection.

References

1. Leon R, Fabelo H, Ortega S, Cruz-Guerrero IA, Campos-Delgado DU, Szolna A, Piñeiro JF, Espino C, O'Shanahan AJ, Hernandez M, Carrera D, Bisshopp S, Sosa C, Balea-Fernandez FJ, Morera J, Clavo B, Callico GM. Hyperspectral imaging benchmark based on machine learning for intraoperative brain tumour detection. NPJ Precis Oncol. 2023 Nov 14;7(1):119. doi: 10.1038/s41698-023-00475-9. PMID: 37964078; PMCID: PMC10646050.
2. Martinez B, Leon R, Fabelo H, Ortega S, Piñeiro JF, Szolna A, Hernandez M, Espino C, J O'Shanahan A, Carrera D, Bisshopp S, Sosa C, Marquez M, Camacho R, Plaza ML, Morera J, M Callico G. Most Relevant Spectral Bands Identification for Brain Cancer Detection Using Hyperspectral Imaging. Sensors (Basel). 2019 Dec 12;19(24):5481. doi: 10.3390/s19245481. PMID: 31842410; PMCID: PMC6961052.
3. Fabelo H, Ortega S, Ravi D, Kiran BR, Sosa C, Bulters D, Callicó GM, Bulstrode H, Szolna A, Piñeiro JF, Kabwama S, Madroñal D, Lazcano R, J-O'Shanahan A, Bisshopp S, Hernández M, Báez A, Yang GZ, Stanciulescu B, Salvador R, Juárez E, Sarmiento R. Spatio-spectral classification of hyperspectral images for brain cancer detection during surgical operations. PLoS One. 2018 Mar 19;13(3):e0193721. doi: 10.1371/journal.pone.0193721. PMID: 29554126; PMCID: PMC5858847.
4. Fabelo H, Ortega S, Lazcano R, Madroñal D, M Callicó G, Juárez E, Salvador R, Bulters D, Bulstrode H, Szolna A, Piñeiro JF, Sosa C, J O'Shanahan A, Bisshopp S, Hernández M, Morera J, Ravi D, Kiran BR, Vega A, Báez-Quevedo A, Yang GZ, Stanciulescu B, Sarmiento R. An Intraoperative Visualization System Using Hyperspectral Imaging to Aid in Brain Tumor Delineation. Sensors (Basel). 2018 Feb 1;18(2):430. doi: 10.3390/s18020430. PMID: 29389893; PMCID: PMC5856119.
5. D. U. Campos-Delgado et al., "Extended Blind End-Member and Abundance Extraction for Biomedical Imaging Applications," in IEEE Access, vol. 7, pp. 178539-178552, 2019, doi: 10.1109/ACCESS.2019.2958985.
6. Anitha, R. and Raja, D. (2017). Development of computer-aided approach for brain tumor detection using random forest classifier. International Journal of Imaging Systems and Technology, 28(1), 48-53. https://doi.org/10.1002/ima.22255
7. Fei, B., Akbari, H., & Halig, L. (2012). Hyperspectral imaging and spectral-spatial classification for cancer detection.. https://doi.org/10.1109/bmei.2012.6513047
8. Gopalachari, M., Kolla, M., Mishra, R., & Tasneem, Z. (2022). Design and implementation of brain tumor segmentation and detection using a novel woelfel filter and morphological segmentation. Complexity, 2022, 1-9. https://doi.org/10.1155/2022/6985927

9. K.S, A., Sobana, J., B, E., Kathiravan, M., & Gopalakrishnan., S. (2019). Automatic brain tissue segmentation using modified k-means algorithm based on image processing techniques.
10. Ma, T., Liu, Y., Huang, W., Wang, C., & Ge, S. (2022). Hyperspectral remote sensing image semantic segmentation using extended extrema morphological profiles..
11. Mridha, K., Simanta, S., & Limbu, N. (2022). U-net for medical imaging: a novel approach for brain tumor segmentation. Global Journal of Innovation and Emerging Technology, 1(1), 20-28. https://doi.org/10.58260/j.iet.2202.0104
12. Noureen, E. and Hassan, M. (2014). Brain tumor detection using histogram thresholding to get the threshold point. Iosr Journal of Electrical and Electronics Engineering, 9(5), 14-19. https://doi.org/10.9790/1676-09531419